

1 **New insights into the reconstructed temperature in Portugal**
2 **over the last 400-years**

3 **J. A. Santos¹, M. F. Carneiro¹, A. Correia², M. J. Alcoforado³, E. Zorita⁴, J. J.**
4 **Gómez-Navarro⁵**

5 [1] {Centre for the Research and Technology of Agro-Environmental and Biological
6 Sciences, CITAB, Universidade de Trás-os-Montes e Alto Douro, UTAD, 5000-801 Vila
7 Real, Portugal }

8 [2] {Department of Physics and Geophysical Centre of Évora, University of Évora, Évora,
9 Portugal }

10 [3] {Centro de Estudos Geográficos, IGOT, Universidade de Lisboa, Ed. Faculdade de Letras,
11 1600-214 Lisboa, Portugal }

12 [4] {Institute for Coastal Research, Helmholtz-Zentrum Geesthacht, Geesthacht, Germany }

13 [5] {Climate and Environmental Physics, Physics Institute and Oeschger Centre for Climate
14 Change Research, University of Bern, 3012 Bern, Switzerland }

15

16 Correspondence to: J. A. Santos (jsantos@utad.pt);

17

18 **Abstract**

19 The [consistency](#) of an existing reconstructed annual (December–November) temperature series
20 for the Lisbon region (Portugal) from 1600 onwards, based on a European-wide reconstruction,
21 with: (1) five local borehole temperature-depth profiles; (2) synthetic temperature-depth
22 profiles, generated from both reconstructed temperatures and two regional paleoclimate
23 simulations in Portugal; (3) instrumental data sources over the twentieth century; and (4)
24 temperature indices from documentary sources during the late Maunder Minimum (1675–1715)
25 is assessed. [The low-frequency variability of the reconstructed temperature in Portugal is not](#)
26 [entirely consistent with local borehole temperature-depth profiles and with the simulated](#)
27 [response of temperature in two regional paleoclimate simulations driven by reconstructions of](#)
28 [various climate forcings](#). Therefore, the existing reconstructed series is calibrated by adjusting
29 its low-frequency variability to the simulations (first-stage adjustment). The annual
30 reconstructed series is then calibrated in its location and scale parameters, using the
31 instrumental series and a linear regression between them (second-stage adjustment). This
32 calibrated series shows clear footprints of the Maunder and Dalton minima, commonly related
33 to changes in solar activity and explosive volcanic eruptions, and a strong recent-past warming,
34 commonly related to human-driven forcing. Lastly, it is also in overall agreement with annual
35 temperature indices over the late Maunder Minimum in Portugal. The series resulting from this
36 post-reconstruction adjustment can be of foremost relevance to improve the current
37 understanding of the driving mechanisms of climate variability in Portugal.

38

39 **Keywords:** Reconstructed temperature, borehole climatology, paleoclimate simulations,
40 historical climatology, non-linear long-term trend, Portugal

41

42 **1. Introduction**

43 Climate reconstructions allow further insight into the climatic variability beyond the relatively
44 short instrumental period, being commonly based on early instrumental records, documentary
45 evidence, namely memoirs, diaries, chronicles, weather logs, ship logbooks, and natural
46 proxies, such as boreholes, tree-rings, corals, ice-cores, speleothem records, pollen-profiles
47 (Brázdil et al., 2010; Brázdil et al., 2005; Camuffo et al., 2010; Li et al., 2010; Luterbacher et
48 al., 2006; Pollack and Huang, 2000). Historical climatology is critical for understanding the
49 driving processes of climate variability not only in the past, but also in the future. This is
50 particularly important when developing climate change projections for the future under
51 emission scenarios (IPCC, 2013).

52 Climate variability in Europe over the last millennium was reconstructed based on both
53 documentary evidence and natural proxies (e.g. Alcoforado et al., 2000; Brázdil et al., 2010;
54 Brázdil et al., 2005; Camuffo et al., 2013; González-Rouco et al., 2009; Luterbacher et al.,
55 2006). European-wide temperature reconstructions since 1500 were already developed
56 (Luterbacher et al., 2004; Xoplaki et al., 2005), as well as continental-wide reconstructions for
57 the last two millennia by Ahmed et al. (2013). Temperature reconstructions in some European
58 sites, based on both documentary data and instrumental records since the 16th century, were
59 carried out by Camuffo et al. (2010). A temperature reconstruction for southern Portugal during
60 the late Maunder Minimum (LMM; 1675-1715) was presented by Alcoforado et al. (2000).
61 However, in Portugal, most of the pre-instrumental records show numerous temporal gaps and
62 there is a substantial lack of natural proxies with clear climatic signals (Alcoforado et al., 2012;
63 Camuffo et al., 2010; Luterbacher et al., 2006).

64 Borehole temperature-depth profiles can be used as paleoclimate proxies for climate
65 reconstruction (e.g. Bodri and Čermák, 1997; González-Rouco et al., 2009; Majorowicz et al.,
66 1999; Šafanda et al., 2007), as they provide independent information on long-term temperature
67 variability (Jones et al., 2009). Borehole measurements are a complementary temperature
68 record to high-frequency air temperature series recorded at weather stations and, through profile
69 inversion methods, may also enable validating low-frequency variability in these series (e.g.
70 Beltrami and Bournon, 2004; Beltrami and Mareschal, 1995; Beltrami et al., 2011; Chouinard
71 and Mareschal, 2007; González-Rouco et al., 2006; Gouirand et al., 2007; Harris and Chapman,
72 1998; Harris and Gosnold, 1999; Nielsen and Beck, 1989; Pollack et al., 2006). Some studies
73 have been carried out using borehole temperature logs measured in southern Portugal (e.g.

74 Correia and Šafanda, 2001; Correia and Šafanda, 1999; Šafanda et al., 2007). Borehole
75 reconstructions can also be compared to paleoclimate simulations generated by Earth system
76 models for validation purposes (Beltrami et al., 2006; González-Rouco et al., 2009; Stevens et
77 al., 2008).

78 The present study aims at analysing the consistency between the Luterbacher et al. (2004) and
79 Xoplaki et al. (2005) temperature reconstructions for the Lisbon region (Portugal) and over the
80 period of 1600–1999 using: 1) five local borehole temperature-depth profiles; 2) synthetic
81 temperature-depth profiles, generated from gridded near-surface temperatures produced by
82 regional paleoclimate reconstructions and simulations; 3) instrumental data recorded in Lisbon
83 over the twentieth century; and 4) temperature indices from early instrumental and documentary
84 sources during the LMM (1675-1715). This analysis allows a validation of the annual mean
85 reconstructed temperature in Portugal over the last 400 years. The identification of possible
86 inconsistencies with the above-referred data sources enables a post-reconstruction adjustment
87 of this time series. In effect, this calibrated time series may help understanding past climate
88 variability in Portugal and its main driving mechanisms, namely the role of external vs. internal
89 forcing mechanisms on temperature variability. This attribution analysis provides critical
90 information for model validation and for assessing the reliability of regional climate change
91 projections. The datasets and methods are presented in section 2, the results are discussed in
92 section 3 and the main conclusions are summarized in section 4.

93

94 **2. Data and Methods**

95 **2.1 Reconstructed temperatures**

96 The reconstructed seasonal mean temperature in the gridbox (38.5–39.0°N, 8.0–8.5°W), which
97 is located in the area of Lisbon (Portugal), and for the period of 1600-1999 was extracted from
98 the Luterbacher et al. (2004) and Xoplaki et al. (2005) European-wide reconstructions (Lut2004
99 henceforth). Data is originally defined on a 0.5° latitude × 0.5° longitude grid. From 1901
100 onwards this dataset is based on instrumental data from New et al. (2000). For the selected
101 gridbox, it is largely based on temperature records from Lisbon. Since the present study focuses
102 on annual series, annual mean temperatures were obtained by averaging the four values
103 corresponding to winter (DJF), spring (MAM), summer (JJA) and autumn (SON) mean
104 temperatures (no monthly data is available). Hence, annual means refer to the period from

105 December of the previous year to November of that year (e.g. annual mean of 1710 corresponds
106 to the average taken from December 1709 to November 1710).

107

108 **2.2 Borehole data**

109 The consistency of the Lut2004 reconstruction with borehole measurements, retrieved from the
110 only geothermal-paleoclimatological observatory in Portugal (38.34° N; 7.58° W), is assessed.
111 [This observatory](#) is located about 5 km northwestwards of Évora (southern Portugal) and about
112 100 km eastwards of Lisbon. More detailed information can be found in Correia and Šafanda
113 (2001) and Šafanda et al. (2007). Although the borehole measurements were not taken in
114 Lisbon, the variability in the 11-yr moving averages of annual mean temperatures in Évora and
115 Lisbon is quite similar (not shown). In fact, the correlation coefficient is of about 0.98 in their
116 common instrumental period (1941-1999). The means for Lisbon and Évora are of 16.8°C and
117 15.8°C, respectively, while both standard deviations are of ca. 0.3°C. Hence, these borehole
118 measurements are assumed to be representative of the measurements made in Lisbon, as they
119 mostly capture long-term variability.

120 Five measurements (temperature logs) in the same borehole TGQC1 are considered herein,
121 which were carried out on 24 March 1997 (M1), 27 March 2000 (M2), 14 November 2002
122 (M3), 26 November 2003 (M4), and 28 October 2004 (M5), respectively. These five
123 temperature logs were obtained by measuring the equilibrium temperature with a thermistor
124 every 5.0 m (M1), 1.0 m (M2), 2.5 m (M3 and M4) and 2.0 m (M5), along the ~190 m depth in
125 the borehole. The borehole is located in a region where the typical vegetation is old cork trees.
126 This vegetation type has not changed in the last hundred years and the topography is subdued,
127 with small elevation variations of tens of meters in the nearest few kilometres. The rock type in
128 the area is hercynian age granite. Its thermophysical properties were measured in four samples,
129 collected in a quarry located in the same granitic body and 1.5 km eastwards of the borehole.
130 Thermal conductivity values of $2.8 \pm 0.2 \text{ W mK}^{-1}$ and thermal diffusivity values of 1.3 ± 0.1
131 $\text{m}^2 \text{ s}^{-1}$ were measured on polished surfaces of rock samples. Heat production was calculated as
132 $2 \pm 1 \text{ W m}^{-3}$ (Correia and Šafanda, 2001). The estimated heat flux density for the borehole is
133 60 mW m^{-2} , which was confirmed as an *a posteriori* value of $58 \pm 13 \text{ mW m}^{-2}$ using the
134 Functional Space Inversion method of Shen and Beck (1992).

135 The borehole temperature-depth profiles are herein compared to synthetic temperature profiles
136 (forward model), generated from both Lut2004 and annual mean near-surface temperatures

137 from **two** paleoclimate simulations, rather than applying the conventional procedure of
 138 inverting temperature logs to reconstruct ground surface temperatures (e.g. Correia and
 139 Šafanda, 2001). However, the uncertainties inherent to these inversion models (Hartmann and
 140 Rath, 2005), mostly due to errors in the estimation of subsurface parameters, are also present
 141 in these forward models. The profiles were generated following the methodology described by
 142 Beltrami et al. (2011), as explained below.

143 The temperature anomaly at depth z and time t , due to a step change in surface temperature T_0 ,
 144 is given by the solution of the one-dimensional heat diffusion equation (Carslaw and Jaeger,
 145 1959):

$$146 \quad T(z,t) = T_0 \operatorname{erfc}\left(\frac{z}{2\sqrt{kt}}\right), \quad (1)$$

147 where erfc is the complementary error function and k is the subsurface thermal diffusivity
 148 (Cermak and Rybach, 1982). It has a value of $1.3 \times 10^{-6} \text{ m}^2\text{s}^{-1}$, according to measurements on
 149 cut and polished surfaces of local rock samples (Correia and Šafanda, 2001). Generalizing this
 150 solution for a series of K step changes at the surface, the induced temperature anomalies at
 151 depth z are given by Mareschal and Beltrami (1992):

$$152 \quad T_i(z) = T_i(z) + \sum_{j=1}^K T_j \left[\operatorname{erfc}\left(\frac{z}{2\sqrt{kt_j}}\right) - \operatorname{erfc}\left(\frac{z}{2\sqrt{kt_{j-1}}}\right) \right], \quad (2)$$

153 where $T_i(z)$ is the initial temperature profile.

154

155 **2.3 Paleoclimate simulations**

156 The **two** paleoclimate simulations were carried out with the Global Circulation Model (GCM)
 157 – ECHO-G, and then dynamically downscaled with the Regional Climate Model (RCM) –
 158 MM5. ECHO-G combines the HOPE-G ocean model (Legutke and Voss, 1999) with the
 159 ECHAM4 atmospheric model (Roeckner et al., 1996). The regional model employs a limited
 160 area domain that spans completely the Iberian Peninsula with a spatial resolution of 30 km.
 161 Three reconstructed external forcings were used to consistently drive both models: solar
 162 variability, atmospheric greenhouse gas concentrations and radiative effects of stratospheric
 163 volcanic aerosols. The skill of the MM5/ECHO-G setup to reproduce the climate in the Iberian
 164 Peninsula has been previously evaluated by Gómez-Navarro et al. (2011), particularly with

165 respect to the ability of the regional model to reduce the warm bias and to correct the winter
166 variability over western Iberia in the GCM run. Two paleoclimate simulations (Sim1 and Sim2),
167 only differing in their initial conditions, were used as a broad estimation of the effect of internal
168 variability (cf. Gómez-Navarro et al., 2012; González-Rouco et al., 2003; Zorita et al., 2007;
169 Zorita et al., 2005). Near-surface (2 m) temperatures for the period of 1600-1989 are extracted
170 from these simulations. Their daily mean fields were bilinearly interpolated from the original
171 MM5 grid to the reconstructed temperature grid (0.5° latitude \times 0.5° longitude) and extracted
172 for the above-defined Lisbon gridbox ($38.5\text{--}39.0^\circ\text{N}$, $8.0\text{--}8.5^\circ\text{W}$). Annual (December–
173 November) means were then computed from the raw 6-hourly data.

174 In order to identify low-frequency variability and trends in the paleoclimate simulations, a data-
175 adaptive filtering, based on a singular spectral analysis (SSA), is applied (Ghil and Vautard,
176 1991). SSA is based on the well-known principal component analysis, in which the multiple
177 dimensionality is achieved by including time-lagged replicas of the original time series. The
178 resulting principal components are thus linear combinations of different lags of this series,
179 which is equivalent to a time filtering with filter-coefficients that are related to the eigenvectors
180 of the lagged-covariance matrix. More formally, SSA corresponds to an eigenvalue
181 decomposition of a lagged-covariance matrix, with a Toeplitz structure, obtained from the
182 original time series of the paleoclimatic simulations. The rank, M , of this matrix is the average
183 of $(N/4\text{--}N/3)$, where N is the time series length (Plaut and Vautard, 1994). For the paleoclimatic
184 simulations $M=113$ ($N=390$). In this methodology, the original time series can also be
185 decomposed into a sum of M additive components and can be partially rebuilt using only the
186 leading ‘signal modes’, thus filtering out background noisy components (Elsner and Tsonis,
187 1996; Vautard et al., 1992). In n -order SSA filtering, the leading n modes are used to rebuild
188 the original time series. The lower the number of retained modes, the stronger is the time series
189 smoothing. If all M modes are used, the original time series is fully recovered.

190 Under the assumption that the aforementioned external forcings used in the paleoclimate
191 simulations are mainly manifested by long-term temperature trends in western Iberia, as
192 suggested by Gómez-Navarro et al. (2012), similar trends of reconstructed and simulated
193 temperatures should be expected. As SSA enables isolating data-adaptive non-linear trends in
194 the time series (Ghil and Vautard, 1991), it can be used to correct discrepancies between long-
195 term trends of reconstructed and simulated temperature series. In the present study, this
196 approach was used to adjust the low-frequency variability in the reconstructed series to the

197 paleoclimate external forcings obtained from the simulations (adjustment of the Lut2004
198 reconstruction). Therefore, instead of developing a new reconstruction, an adjustment of the
199 already existing reconstruction was carried out herein (post-reconstruction adjustment).

200

201 **2.4 Instrumental data and indexed temperatures**

202 The consistency of the Lut2004 reconstruction with the corresponding instrumental series
203 (InstT) for the available period of 1901–1999, recorded at the Lisboa-Geofísico meteorological
204 station and supplied by the European Climate Assessment & Dataset project (Klein Tank et al.,
205 2002), was also assessed. It should be stressed that Lut2004 is heavily dependent on InstT, as
206 previously referred, and a high temporal correspondence between these two time series is
207 thereby expected. A transfer-function between InstT and Lut2004 was determined by using a
208 linear regression analysis. The resulting first-order regression polynomial was applied so as to
209 calibrate the Lut2004 reconstruction in the extended period from 1600 onwards, thus correcting
210 its location and scale parameters. Lastly, annual indexed temperatures for southern Portugal
211 over the pre-instrumental period of 1675–1715 (LMM), developed by Alcoforado et al. (2000),
212 were also analysed for consistency assessment.

213

214 **3. Results**

215 **3.1 Consistency with borehole measurements and paleoclimate simulations**

216 The consistency of the Lut2004 reconstruction with borehole temperature-depth profiles and
217 with paleoclimate simulations is assessed in this section. The five logs of borehole
218 measurements (M1, M2, M3, M4 and M5) are shown in Fig. 1a. Their corresponding inverse
219 geothermal gradients were estimated using linear regressions applied to the bottom 140–180 m
220 data (Fig. 1b). Owing to the deposition of fine material at the bottom of the borehole, there is
221 locally a change in thermal conductivity at about 180 m. As the borehole was drilled in a very
222 homogeneous granite batholith, these changes are not due to changes in the geological
223 formation. In the present study, depths >180m are not used for gradient estimations. These
224 gradients approximately range from 46 to 48 m °C⁻¹ (ca. 0.021 °C m⁻¹). The corresponding root-
225 mean squared error (RMSE) of each estimated linear model is always <0.01°C (R-square
226 adjusted >99.9%), which means that the errors in the estimation of the geothermal gradients
227 have only minor impacts on the subsequent temperature-depth anomalies. The low borehole

228 depths require a word of caution, as some authors have indicated that 200 m of depth may be
229 too shallow for climate change assessments (Beltrami et al., 2011; Hamza et al., 2007;
230 Majorowicz et al., 1999). The Global Database of Borehole Temperatures and Climate
231 Reconstructions from the University of Michigan and the World Data Center for
232 Paleoclimatology indeed consider a 200 m depth as a minimum requirement for past climate
233 reconstruction (Pollack and Huang, 2000). Beltrami et al. (2011) also demonstrated that the
234 maximum depth of borehole profiles can have a large impact on temperature-depth anomalies.
235 Since no other geothermal-paleoclimatological observatory is available in Portugal, the
236 conclusions derived from these borehole profiles may be provisional.

237 The five temperature-depth anomaly profiles (M1–5), after removing their estimated
238 geothermal gradients, are reproduced in Fig. 2a. M1, M2, M3 and M4 show a more pronounced
239 near-surface warming than M5. Overall, these profiles suggest strong recent-past warming
240 trends in near-surface air temperatures.

241 The synthetic temperature-depth anomaly profiles, generated from the Lut2004 reconstruction
242 and from the two paleoclimate simulations, are also shown in Fig. 2a. The 11-year running
243 means of their anomalies over the period 1600–1989 are plotted in Fig. 2b. The chronograms
244 of the two simulations, as well as their individual profiles, are indeed very similar to the
245 corresponding ensemble mean chronograms and profiles (not shown). In fact, the correlation
246 coefficient between the 11-yr running means of the two simulations is as high as +0.82. This is
247 indicative of the large influence of external forcings in the long-term variability of temperature.
248 Conversely to the simulations, which exhibit a strong warming trend since the 1830s, Lut2004
249 only depicts a recent-past upward trend and a cooling trend during the nineteenth century (Fig.
250 2b). Although the recent-past warming trend in Lut2004 is clearly corroborated by InstT, the
251 cooling trend is neither supported by simulations (Fig. 2b) nor by any scientific evidence from
252 previous studies. As a result, the synthetic temperature-depth anomaly profile obtained from
253 Lut2004 is clearly different from the profiles obtained from the five borehole measurements
254 and from the paleoclimate simulations (Fig.2a).

255 The discussion above hints at a remarkable agreement between the low-frequency variability
256 of near-surface temperature from two independent sources (borehole measurements and
257 paleoclimate simulations driven by reconstructed forcing). However, whereas the paleoclimate
258 simulations agree well with the borehole temperature-depth profiles, the reconstructed
259 temperature for Portugal (Lut2004) is not entirely consistent with the long-term trends revealed

260 by these new sources. In fact, its linear trend is nearly zero over the whole period and there is
261 no signature of cool/warm periods. This disagreement between simulations and Lut2004 was
262 already reported by Gómez-Navarro et al. (2011). As such, the low-frequency variability of the
263 Lut2004 reconstruction are herein adjusted to be more coherent with the borehole data and
264 simulations. Towards this aim, the ensemble mean temperature from the two simulations was
265 low-pass filtered by a 2-order SSA. The filtered series (SSA-trend in Fig. 2b) highlights the
266 signature of the external forcings on near-surface temperature and was then added to the
267 Lut2004 reconstruction. The resulting calibrated series (CalT = Lut2004 + SSA-trend) is also
268 shown in Fig. 2b.

269 The SSA-trend clearly shows a warming trend since the 1830s and a relatively cool period
270 during the LMM (1670–1730). This is also in line with previous studies on the impact of solar
271 activity on global temperatures (e.g. Eddy, 1983; Frenzel, 1994). The period from 1730 to 1800
272 recorded annual mean temperatures close to the baseline, being followed by an anomalously
273 cold period until the 1830s, which is associated with the Dalton Minimum, also a period of low
274 solar activity (Wagner and Zorita, 2005). The strong upward trend in CalT from the 1830s
275 onwards is now in clear agreement with the paleoclimate simulations and InstT (in the twentieth
276 century). The LMM (ca. 1670–1730) and Dalton minimum (ca. 1790–1830) are also clearly
277 depicted in CalT. Furthermore, the temperature-depth anomaly profile from CalT is similar to
278 the profiles from the five borehole measurements and paleoclimate simulations (Fig. 2a). This
279 represents an important validation of CalT.

280

281 3.2 Consistency with instrumental data

282 The consistency between InstT and CalT has been assessed by a linear regression in their
283 common period (1901–1989). The corresponding scatterplot shows that linear regression
284 provides a good fitting, with a correlation coefficient above 0.90 (Fig. 3), explaining about 82%
285 of the total variance (R-square adjusted), and a RMSE of 0.22. According to the Fisher's test,
286 this least-squares linear regression model is statistically significant at a 99% confidence level
287 ($p < 0.01$). A bootstrap procedure with 10,000 resamples shows that the 95% confidence interval
288 for the correlation coefficient between InstT and CalT is [0.87, 0.93], supporting the Fisher's
289 test. Therefore, CalT clearly reproduces the observed temperature in Portugal in the
290 instrumental period (InstT). A 3-order polynomial fitting, with a robust regression using the
291 bisquare weighting method, provides a slightly better adjustment (R-square adjusted of 83%

292 and RMSE of 0.21), but its extrapolation for the lowest temperatures (outside the range of
293 values used in the model fitting, not shown) is not reliable and was discarded. The
294 corresponding linear regression polynomial is applied for a second-stage adjustment of location
295 and scale parameters in CalT. This allows expressing CalT in absolute temperature values
296 instead of anomalies (Fig. 4a). Additionally, taking into account the high coherency between
297 CalT and InstT, CalT was extended from 1989 to 1999 using InstT values. In order to confirm
298 long-term trends in CalT, the non-parametric progressive Mann-Kendall test is applied
299 (Sneyers, 1990, 1992). The forward and backward Kendall t parameters for CalT jointly depict
300 a warming trend from the 1830s onwards, being particularly noteworthy since the 1930s
301 (Fig.4b).

302 The uncertainties in the CalT series are a combination of the original uncertainties in the
303 Lut2004 dataset plus additional uncertainties related to the non-linear trend used in the
304 adjustment. The former are discussed in Luterbacher et al. (2004), [but are only available for the](#)
305 [European mean reconstruction. Hence, it is not possible to have a local estimate of these](#)
306 [uncertainties](#). The latter can be estimated through the assessment of the consistence between
307 Sim1 and Sim2. For this purpose, the SSA filtering was applied separately to Sim1 and Sim2.
308 The mean absolute difference between the two non-linear trends obtained from Sim1 and Sim2
309 provides a measure of the uncertainty related to the simulations. It has an approximate value of
310 0.05°C. However, this number provides just a lower bound, since it does not explicitly consider
311 uncertainties related to the simulation itself, which are difficult to assess due to the limited
312 number of available simulations with similar characteristics.

313

314

315 **3.3 Consistency with precipitation indices**

316 In previous studies, temperature in southern Portugal was analysed during the LMM (1675–
317 1715) by Alcoforado et al. (2000), and during the eighteenth century by Taborda et al. (2004)
318 and Alcoforado et al. (2012). In these studies, research was based on documentary evidence,
319 such as diaries, ecclesiastical rogation ceremonies (*pro-pluvia* and *pro-serenitate*),
320 *Misericórdias* and municipal institutional sources, as well as on early instrumental data. From
321 this documentary evidence, basic data were transformed into indices on an ordinal scale,
322 following the methodology developed by Pfister (1995). Monthly temperatures were originally
323 indexed on a scale from 0 to ± 1 . Annual indices (December–November) can then vary from 0

324 to ± 12 . The consistency between CalT and the corresponding annual indexed temperatures is
325 assessed by their respective scatterplots (Fig. 5). For a perfect agreement, the documented
326 temperature extremes (cold/hot years) should be reflected by coherent CalT anomalies, i.e. all
327 data pairs in the scatterplots should be either on top-right or bottom-left quadrants (positively
328 aligned series). There is an overall agreement between CalT and [the annual temperature index](#)
329 ($>80\%$ of all years are on top-right or bottom-left quadrants, with a correlation coefficient of
330 0.76). Therefore, this agreement also provides a validation of CalT for the period of 1675–1715.
331 [However, as the SSA-filtering does not significantly modify the interannual variability within](#)
332 [this relatively short time period \(LMM\), the aforementioned agreement also applies between](#)
333 [Lut2004 and the annual temperature index \(not shown\).](#)

334

335 **4. Summary and conclusions**

336 The consistency of the reconstructed annual temperature series in Portugal (Lut2004) is
337 assessed by using five borehole temperature-depth profiles, synthetic temperature-depth
338 profiles generated from both the Lut2004 reconstruction and paleoclimate simulations,
339 instrumental data (InstT) and indexed temperatures during the LMM. While the paleoclimate
340 simulations agree well [in the long-term variability](#) with the borehole temperature-depth profiles,
341 the same does not apply to the Lut2004 reconstruction. In fact, [the long-term trends in Lut2004](#)
342 [are not fully consistent with borehole data and simulations.](#) The late Maunder and Dalton
343 minima, clearly reflected in the paleoclimate simulations and well-documented in the literature,
344 in association with changes in solar activity (Eddy, 1983), are absent from the Lut2004
345 reconstruction. Moreover, there is a cooling trend throughout the nineteenth century that is not
346 supported by previous studies. Therefore, the Lut2004 reconstruction was calibrated by
347 adjusting its low-frequency variability to the paleoclimatic simulations, also in agreement with
348 local borehole data. Documentary sources in Portugal during the LMM (1675–1715) also show
349 high agreement with CalT, thus providing an additional validation over the LMM.

350 [These results suggest some inconsistencies in the low-frequency variability of temperature in](#)
351 [Portugal between the Lut2004 reconstruction and borehole data or simulations.](#) In effect, the
352 absence of clear long-term trends in Lut2004 is not coherent with the significant changes in the
353 radiative forcing throughout the last 400 years and the important role played by these external
354 forcings on temperature variability over western Iberia (Gómez-Navarro et al., 2012). The
355 frequent temporal gaps in the pre-instrumental records and the substantial lack of natural

356 proxies with clear climatic signals in Portugal (Alcoforado et al., 2012; Camuffo et al., 2010;
357 Luterbacher et al., 2006) may partially explain [this limitation in the reproduction](#) of the low-
358 frequency variability in the Lut2004 reconstruction. [An important](#) loss of low-frequency
359 variance caused by the method used in Lut2004 was also found by von Storch et al. (2009).
360 Nevertheless, a more detailed assessment of the causes for this shortcoming is out of the scope
361 of the present study, as it does not develop a new reconstruction for comparison, but rather an
362 adjustment of an existing reconstruction.

363 [CaIT adjusts the low-frequency variability in the Lut2004 reconstruction so as to be more](#)
364 [consistent with local borehole measurements and regional climate simulations](#). It can thus be of
365 foremost relevance in forthcoming research on climatic variability in Portugal. [A reliable](#)
366 [representation of the low-frequency variability of temperature in Portugal, including its long-](#)
367 [term trends, is critical for understanding the role played by external vs. internal forcings on the](#)
368 [regional climate variability and change](#). Due to the relatively coarse spatial resolution of data
369 generated by state-of-the-art GCMs, they are not suitable for regional-scale assessments. Since
370 such scales are precisely the focus of this study, temperature series from two high-resolution
371 regional paleoclimatic simulations (Sim1 and Sim2) are employed instead of GCM runs. These
372 two simulations were documented and validated in previous studies. Unfortunately, there are
373 only two available simulations covering Portugal with such high-resolution characteristics.
374 Hence, it is not possible to increase the ensemble size of model simulations, though it would be
375 very useful for uncertainty assessments. In forthcoming research, new regional paleoclimatic
376 simulations over Portugal, also using different models, should be used to enhance the robustness
377 and evaluate the significance of the current adjustment.

378

379 *Acknowledgements.* This study was carried out within the framework of the project
380 ‘Reconstruction and model simulations of past climate in Portugal, using documentary and
381 early instrumental sources – Klimhist’ and was supported by national funds from FCT -
382 Portuguese Foundation for Science and Technology [PTDC/AAC-CLI/119078/2010] and
383 [\[UID/AGR/04033/2013\]](#).

384

385 **References**

- 386 Ahmed, M., Anchukaitis, K. J., Asrat, A., Borgaonkar, H. P., Braida, M., Buckley, B. M.,
387 Buntgen, U., Chase, B. M., Christie, D. A., Cook, E. R., Curran, M. A. J., Diaz, H. F., Esper,
388 J., Fan, Z. X., Gaire, N. P., Ge, Q. S., Gergis, J., Gonzalez-Rouco, J. F., Goosse, H., Grab, S.
389 W., Graham, N., Graham, R., Grosjean, M., Hanhijarvi, S. T., Kaufman, D. S., Kiefer, T.,
390 Kimura, K., Korhola, A. A., Krusic, P. J., Lara, A., Lezine, A. M., Ljungqvist, F. C., Lorrey,
391 A. M., Luterbacher, J., Masson-Delmotte, V., McCarroll, D., McConnell, J. R., McKay, N. P.,
392 Morales, M. S., Moy, A. D., Mulvaney, R., Mundo, I. A., Nakatsuka, T., Nash, D. J., Neukom,
393 R., Nicholson, S. E., Oerter, H., Palmer, J. G., Phipps, S. J., Prieto, M. R., Rivera, A., Sano, M.,
394 Severi, M., Shanahan, T. M., Shao, X. M., Shi, F., Sigl, M., Smerdon, J. E., Solomina, O. N.,
395 Steig, E. J., Stenni, B., Thamban, M., Trouet, V., Turney, C. S. M., Umer, M., van Ommen, T.,
396 Verschuren, D., Viau, A. E., Villalba, R., Vinther, B. M., von Gunten, L., Wagner, S., Wahl, E.
397 R., Wanner, H., Werner, J. P., White, J. W. C., Yasue, K., Zorita, E., and Consortium, P. k.:
398 Continental-scale temperature variability during the past two millennia, *Nat. Geosci.*, 6, 339-
399 346, doi:10.1038/Ngeo1797, 2013.
- 400 Alcoforado, M. J., Nunes, M. F., Garcia, J. C., and Taborda, J. P.: Temperature and precipitation
401 reconstruction in southern Portugal during the late Maunder Minimum (AD 1675–1715),
402 *Holocene*, 10, 333–340, 2000.
- 403 Alcoforado, M. J., Vaquero, J. M., Trigo, R. M., and Taborda, J. P.: Early Portuguese
404 meteorological measurements (18th century), *Clim. Past*, 8, 353–371, doi:10.5194/cp-8-353-
405 2012, 2012.
- 406 Beltrami, H. and Boursillon, E.: Ground warming patterns in the Northern Hemisphere during the
407 last five centuries, *Earth Planet. Sc. Lett.*, 227, 169–177, 2004.
- 408 Beltrami, H. and Mareschal, J.-C.: Resolution of ground temperature histories inverted from
409 borehole temperature data, *Global Planet. Change*, 11, 57–70, 1995.
- 410 Beltrami, H., González-Rouco, J. F., and Stevens, M. B.: Subsurface temperatures during the
411 last millennium: model and observation, *Geophys. Res. Lett.*, 33, L09705,
412 doi:10.1029/2006GL026050, 2006.
- 413 Beltrami, H., Smerdon, J. E., Matharoo, G. S., and Nickerson, N.: Impact of maximum borehole
414 depths on inverted temperature histories in borehole paleoclimatology, *Clim. Past*, 7, 745–756,
415 doi:10.5194/cp-7-745-2011, 2011.
- 416 Bodri, L. and Čermák, V.: Reconstruction of remote climate changes from borehole
417 temperatures, *Global Planet. Change*, 15, 47-57, doi:10.1016/S0921-8181(97)00004-0, 1997.
- 418 Brázdil, R., Dobrovolný, P., Luterbacher, J., Moberg, A., Pfister, C., Wheeler, D., and Zorita,
419 E.: European climate of the past 500 years: new challenges for historical climatology, *Climatic*
420 *Change*, 101, 7-40, doi:10.1007/s10584-009-9783-z, 2010.
- 421 Brázdil, R., Pfister, C., Wanner, H., Storch, H., and Luterbacher, J.: Historical Climatology In
422 Europe – The State Of The Art, *Climatic Change*, 70, 363-430, doi:10.1007/s10584-005-5924-
423 1, 2005.

- 424 Camuffo, D., Bertolin, C., Barriendos, M., Dominguez-Castro, F., Cocheo, C., Enzi, S.,
425 Sghedoni, M., Valle, A., Garnier, E., Alcoforado, M. J., Xoplaki, E., Luterbacher, J., Diodato,
426 N., Maugeri, M., Nunes, M. F., and Rodriguez, R.: 500-year temperature reconstruction in the
427 Mediterranean Basin by means of documentary data and instrumental observations, *Climatic*
428 *Change*, 101, 169-199, doi:10.1007/s10584-010-9815-8, 2010.
- 429 Camuffo, D., Bertolin, C., Diodato, N., Cocheo, C., Barriendos, M., Dominguez-Castro, F.,
430 Garnier, E., Alcoforado, M. J., and Nunes, M. F.: Western Mediterranean precipitation over the
431 last 300 years from instrumental observations, *Climatic Change*, 117, 85-101,
432 doi:10.1007/s10584-012-0539-9, 2013.
- 433 Carslaw, H. S. and Jaeger, J. C.: *Conduction of Heat in Solids*, Oxford Univ. Press, New York,
434 1959.
- 435 Cermak, V. and Rybach, L.: Thermal conductivity and specific heat of minerals and rocks. In:
436 Subvolume A, Angenheister, G. (Ed.), *Landolt-Börnstein - Group V Geophysics*, Springer
437 Berlin Heidelberg, 341–343, 1982.
- 438 Chouinard, C. and Mareschal, J. C.: Selection of borehole temperature depth profiles for
439 regional climate reconstructions, *Clim. Past*, 3, 297-313, doi:10.5194/cp-3-297-2007, 2007.
- 440 Correia, A. and Šafanda, J.: Ground surface temperature history at a single site in southern
441 Portugal reconstructed from borehole temperatures, *Global Planet. Change*, 29, 155-165,
442 doi:10.1016/S0921-8181(01)00087-X, 2001.
- 443 Correia, A. and Šafanda, J.: Preliminary ground surface temperature history in mainland
444 Portugal reconstructed from borehole temperature logs, *Tectonophysics*, 306, 269-275,
445 doi:10.1016/S0040-1951(99)00060-8, 1999.
- 446 Eddy, J. A.: The Maunder Minimum - a Reappraisal, *Sol. Phys.*, 89, 195-207,
447 doi:10.1007/Bf00211962, 1983.
- 448 Elsner, J. B. and Tsonis, A. A.: *Singular spectrum analysis: a new tool in time series analysis*,
449 Plenum Press, New York; London, 1996.
- 450 Frenzel, B.: *Climatic Trends and anomalies in Europe 1675-1715. High resolution spatio-*
451 *temporal reconstructions from direct meteorological observations and proxy data. Methods and*
452 *Results*, Gustav Fisher Verlag. Stuttgart, Jena and New York, 1994.
- 453 Ghil, M. and Vautard, R.: Interdecadal Oscillations and the Warming Trend in Global
454 Temperature Time-Series, *Nature*, 350, 324-327, doi:10.1038/350324a0, 1991.
- 455 Gómez-Navarro, J. J., Montavez, J. P., Jerez, S., Jimenez-Guerrero, P., Lorente-Plazas, R.,
456 Gonzalez-Rouco, J. F., and Zorita, E.: A regional climate simulation over the Iberian Peninsula
457 for the last millennium, *Clim. Past*, 7, 451-472, doi:10.5194/cp-7-451-2011, 2011.
- 458 Gómez-Navarro, J. J., Montávez, J. P., Jiménez-Guerrero, P., Jerez, S., Lorente-Plazas, R.,
459 González-Rouco, J. F., and Zorita, E.: Internal and external variability in regional simulations
460 of the Iberian Peninsula climate over the last millennium, *Clim. Past*, 8, 25-36, doi:10.5194/cp-
461 8-25-2012, 2012.

- 462 González-Rouco, F., von Storch, H., and Zorita, E.: Deep soil temperature as proxy for surface
463 air-temperature in a coupled model simulation of the last thousand years, *Geophys. Res. Lett.*,
464 30, 2116, doi:10.1029/2003GL018264, 2003.
- 465 González-Rouco, J. F., Beltrami, H., Zorita, E., and Stevens, M. B.: Borehole climatology: a
466 discussion based on contributions from climate modeling, *Clim. Past*, 5, 97-127,
467 doi:10.5194/cp-5-97-2009, 2009.
- 468 González-Rouco, J. F., Beltrami, H., Zorita, E., and von Storch, H.: Simulation and inversion
469 of borehole temperature profiles in surrogate climates: Spatial distribution and surface
470 coupling, *Geophys. Res. Lett.*, 33, L01703, doi:10.1029/2005GL024693, 2006.
- 471 Gouirand, I., Moberg, A., and Zorita, E.: Climate variability in Scandinavia for the past
472 millennium simulated by an atmosphere-ocean general circulation model, *Tellus A*, 59, 30-49,
473 doi:10.1111/j.1600-0870.2006.00207.x, 2007.
- 474 Hamza, V. M., Cavalcanti, A. S. B., and Benyosef, L. C. C.: Surface thermal perturbations of
475 the recent past at low latitudes - inferences based on borehole temperature data from Eastern
476 Brazil, *Clim. Past*, 3, 513-526, 2007.
- 477 Harris, R. N. and Chapman, D. S.: Geothermics and climate change: 1. Analysis of borehole
478 temperatures with emphasis on resolving power, *J. Geophys. Res.-Sol. Ea.*, 103, 7363-7370,
479 doi:10.1029/97JB03297, 1998.
- 480 Harris, R. N. and Gosnold, W. D.: Comparisons of borehole temperature–depth profiles and
481 surface air temperatures in the northern plains of the USA, *Geophys. J. Int.*, 138, 541-548,
482 doi:10.1046/j.1365-246X.1999.00884.x, 1999.
- 483 Hartmann, A. and Rath, V.: Uncertainties and shortcomings of ground surface temperature
484 histories derived from inversion of temperature logs, *J. Geophys. Eng.*, 2, 299,
485 doi:10.1088/1742-2132/2/4/S02, 2005.
- 486 IPCC: Climate Change 2013: The Physical Science Basis. Contribution of Working Group I to
487 the Fifth Assessment Report of the Intergovernmental Panel on Climate Change [Stocker, T.F.,
488 D. Qin, G.-K. Plattner, M. Tignor, S.K. Allen, J. Boschung, A. Nauels, Y. Xia, V. Bex and P.M.
489 Midgley (eds.)]. Cambridge University Press, Cambridge, United Kingdom and New York,
490 NY, USA, 1535 pp., 2013.
- 491 Jones, P. D., Briffa, K. R., Osborn, T. J., Lough, J. M., van Ommen, T. D., Vinther, B. M.,
492 Luterbacher, J., Wahl, E. R., Zwiers, F. W., Mann, M. E., Schmidt, G. A., Ammann, C. M.,
493 Buckley, B. M., Cobb, K. M., Esper, J., Goosse, H., Graham, N., Jansen, E., Kiefer, T., Kull,
494 C., Kuttel, M., Mosley-Thompson, E., Overpeck, J. T., Riedwyl, N., Schulz, M., Tudhope, A.
495 W., Villalba, R., Wanner, H., Wolff, E., and Xoplaki, E.: High-resolution palaeoclimatology of
496 the last millennium: a review of current status and future prospects, *Holocene*, 19, 3-49,
497 doi:10.1177/0959683608098952, 2009.
- 498 Klein Tank, A. M. G., Wijngaard, J. B., Können, G. P., Böhm, R., Demarée, G., Gocheva, A.,
499 Mileta, M., Pashiardis, S., Hejkrlik, L., Kern-Hansen, C., Heino, R., Bessemoulin, P., Müller-
500 Westermeier, G., Tzanakou, M., Szalai, S., Pálsdóttir, T., Fitzgerald, D., Rubin, S., Capaldo,
501 M., Maugeri, M., Leitass, A., Bukantis, A., Aberfeld, R., van Engelen, A. F. V., Forland, E.,
502 Mielus, M., Coelho, F., Mares, C., Razuvaev, V., Nieplova, E., Cegnar, T., Antonio López, J.,

- 503 Dahlström, B., Moberg, A., Kirchhofer, W., Ceylan, A., Pachaliuk, O., Alexander, L. V., and
504 Petrovic, P.: Daily dataset of 20th-century surface air temperature and precipitation series for
505 the European Climate Assessment, *Int. J. Climatol.*, 22, 1441-1453, doi:10.1002/joc.773, 2002.
- 506 Legutke, S. and Voss, R.: The Hamburg atmosphere–ocean coupled circulation model ECHOG,
507 Germany DKRZ Tech. Rep. 18, Dtsch. Klimarechenzentrum, Hamburg, 1999.
- 508 Li, B., Nychka, D. W., and Ammann, C. M.: The Value of Multiproxy Reconstruction of Past
509 Climate, *J. Am. Stat. Assoc.*, 105, 883-895, doi:10.1198/jasa.2010.ap09379, 2010.
- 510 Luterbacher, J., Dietrich, D., Xoplaki, E., Grosjean, M., and Wanner, H.: European seasonal
511 and annual temperature variability, trends, and extremes since 1500, *Science*, 303, 1499-1503,
512 doi:10.1126/science.1093877, 2004.
- 513 Luterbacher, J., Xoplaki, E., Casty, C., Wanner, H., Pauling, A., Küttel, M., Rutishauser, T.,
514 Brönnimann, S., Fischer, E., Fleitmann, D., Gonzalez-Rouco, F. J., García-Herrera, R.,
515 Barriendos, M., Rodrigo, F., Gonzalez-Hidalgo, J. C., Saz, M. A., Gimeno, L., Ribera, P.,
516 Brunet, M., Paeth, H., Rimbu, N., Felis, T., Jacobeit, J., Dünkeloh, A., Zorita, E., Guiot, J.,
517 Türkeş, M., Alcoforado, M. J., Trigo, R., Wheeler, D., Tett, S., Mann, M. E., Touchan, R.,
518 Shindell, D. T., Silenzi, S., Montagna, P., Camuffo, D., Mariotti, A., Nanni, T., Brunetti, M.,
519 Maugeri, M., Zerefos, C., Zolt, S. D., Lionello, P., Nunes, M. F., Rath, V., Beltrami, H., Garnier,
520 E., and Ladurie, E. L. R.: Chapter 1 Mediterranean climate variability over the last centuries: A
521 review. In: *Mediterranean climate variability*, P. Lionello, Malanotte-Rizzoli, P., and Boscolo,
522 R. (Eds.), Elsevier, 2006.
- 523 Majorowicz, J. A., Šafanda, J., Harris, R. N., and Skinner, W. R.: Large ground surface
524 temperature changes of the last three centuries inferred from borehole temperatures in the
525 Southern Canadian Prairies, Saskatchewan, *Global and Planet. Change*, 20, 227-241,
526 doi:10.1016/S0921-8181(99)00016-8, 1999.
- 527 Mareschal, J. C. and Beltrami, H.: Evidence for recent warming from perturbed geothermal
528 gradients: examples from eastern Canada, *Clim. Dynam.*, 6, 135-143,
529 doi:10.1007/BF00193525, 1992.
- 530 New, M., Hulme, M., and Jones, P.: Representing twentieth-century space-time climate
531 variability. Part II: Development of 1901-96 monthly grids of terrestrial surface climate, *J.*
532 *Climate*, 13, 2217-2238, 2000.
- 533 Nielsen, S. B. and Beck, A. E.: Heat-Flow Density Values and Paleoclimate Determined from
534 Stochastic Inversion of 4 Temperature Depth Profiles from the Superior Province of the
535 Canadian Shield, *Tectonophysics*, 164, 345-359, 1989.
- 536 Pfister, C.: Monthly temperature and precipitation in central Europe from 1525-1979:
537 quantifying documentary evidence on weather and its effects. In: *Climate since A.D. 1500*,
538 Bradley, R. S. and Jones, P. D. (Eds.), Routledge, London, 1995.
- 539 Plaut, G. and Vautard, R.: Spells of Low-Frequency Oscillations and Weather Regimes in the
540 Northern-Hemisphere, *J. Atmos. Sci.*, 51, 210-236, 1994.
- 541 Pollack, H. N. and Huang, S. P.: Climate reconstruction from subsurface temperatures, *Annu.*
542 *Rev. Earth. Pl. Sc.*, 28, 339-365, doi:10.1146/annurev.earth.28.1.339, 2000.

- 543 Pollack, H. N., Huang, S. P., and Smerdon, J. E.: Five centuries of climate change in Australia:
544 the view from underground, *J. Quaternary Sci.*, 21, 701-706, doi:10.1002/Jqs.1060, 2006.
- 545 Roeckner, E., Arpe, K., Bengtsson, L., Christoph, M., Claussen, M., Dumenil, L., Esch, M.,
546 Giorgetta, M., Schlese, U., and Schulzweida, U.: The atmospheric general circulation model
547 ECHAM4: model description and simulation of present-day climate, Max-Planck-Institut für
548 Meteorologie, Hamburg, Germany Tech. Rep., 218, 1996.
- 549 Šafanda, J., Rajver, D., Correia, A., and Dedecek, P.: Repeated temperature logs from Czech,
550 Slovenian and Portuguese borehole climate observatories, *Clim. Past*, 3, 453-462,
551 doi:10.5194/cp-3-453-2007, 2007.
- 552 Shen, P. Y. and Beck, A. E.: Paleoclimate Change and Heat-Flow Density Inferred from
553 Temperature Data in the Superior Province of the Canadian Shield, *Global and Planetary*
554 *Change*, 98, 143-165, 1992.
- 555 Sneyers, R.: *On the Statistical Analysis of Series of Observations*, Secretariat of the World
556 Meteorological Organization, Geneva, Switzerland, 1990.
- 557 Sneyers, R.: Use and measure of statistical methods for detection of climatic change, in: *Climate*
558 *Change Detection Project. Report on the Informal Planning Meeting on Statistical Procedures*
559 *for Climate Change Detection*, WCDMP, 20, 176–181, Geneva, Switzerland, 1992.
- 560 Stevens, M. B., González-Rouco, J. F., and Beltrami, H.: North American climate of the last
561 millennium: Underground temperatures and model comparison, *J. Geophys. Res.-Earth*, 113,
562 F01008, doi:10.1029/2006JF000705, 2008.
- 563 Taborda, J. P., Alcoforado, M. J., and Garcia, J. C.: Climate in southern Portugal in the 18th
564 century. Reconstruction based on documentary and early instrumental sources (in Portuguese,
565 with extended English summary), University of Lisbon, *Geo-Ecologia*, 2, CEG, Lisboa, ISBN:
566 972-636-144-3, 2004. http://clima.ul.pt/images/pdf/pub/b_mja_2004_climasulportugal.pdf
- 567 Vautard, R., Yiou, P., and Ghil, M.: Singular-Spectrum Analysis - a Toolkit for Short, Noisy
568 Chaotic Signals, *Physica D*, 58, 95-126, 1992.
- 569 von Storch, H., Zorita, E., and Gonzalez-Rouco, F.: Assessment of three temperature
570 reconstruction methods in the virtual reality of a climate simulation, *Int. J. Earth Sci.*, 98, 67-
571 82, doi:10.1007/s00531-008-0349-5, 2009.
- 572 Wagner, S. and Zorita, E.: The influence of volcanic, solar and the Dalton Minimum (1790-
573 1830): CO2 forcing on the temperatures in a model study, *Clim. Dyn.*, 25, 205-218,
574 doi:10.1007/s00382-005-0029-0, 2005.
- 575 Xoplaki, E., Luterbacher, J., Paeth, H., Dietrich, D., Steiner, N., Grosjean, M., and Wanner, H.:
576 European spring and autumn temperature variability and change of extremes over the last half
577 millennium, *Geophys. Res. Lett.*, 32, L15713, doi:10.1029/2005GL023424, 2005.
- 578 Zorita, E., Gonzalez-Rouco, F., and von Storch, H.: Comments on “Testing the Fidelity of
579 Methods Used in Proxy-Based Reconstructions of Past Climate”, *J. Climate*, 20, 3693-3698,
580 doi:10.1175/JCLI4171.1, 2007.

581 Zorita, E., González-Rouco, J. F., von Storch, H., Montávez, J. P., and Valero, F.: Natural and
582 anthropogenic modes of surface temperature variations in the last thousand years, *Geophys.*
583 *Res. Lett.*, 32, L08707, doi:10.1029/2004GL021563, 2005.
584

585 **Figure Captions**

586 **Fig. 1.** (a) Borehole temperature logs (temperature vs. depth) for: M1, M2, M3, M4 and M5 from the Évora
587 observatory (cf. legends). (b) The same as on (a), but only for the bottom 140–180 m data. The outlined equations
588 of the respective regression lines (omitted) represent the corresponding estimated geothermal gradients (slope of
589 the linear regression line).

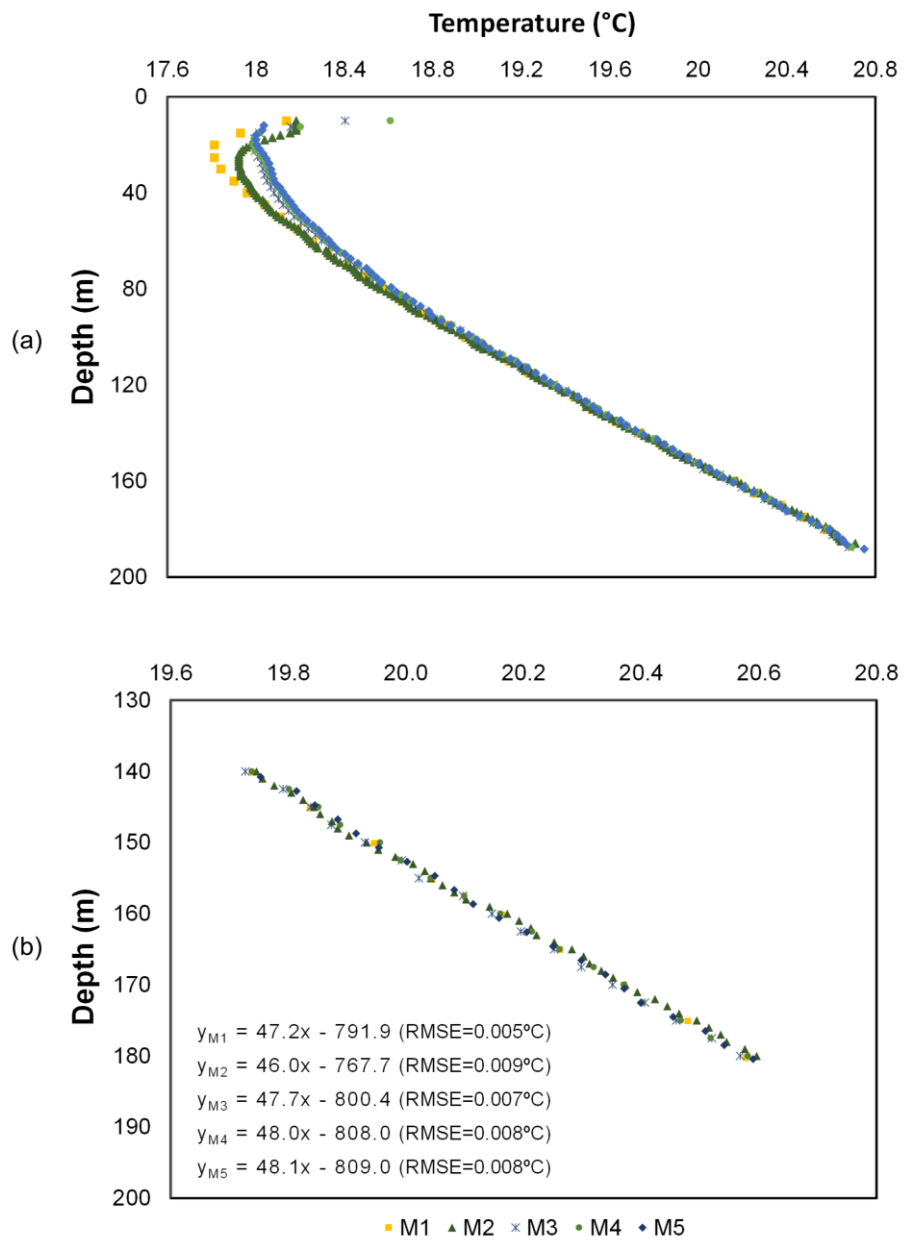
590 **Fig. 2.** (a) Temperature-depth anomaly profiles for: M1, M2, M3, M4 and M5, with respect to the estimated
591 geothermal gradients in Fig. 1b, along with the synthetic profiles generated from: Lut2004 – reconstructed
592 temperature; CalT – calibrated temperature; and Sim1/Sim2 – paleoclimate simulations, retrieved for a gridbox
593 near Lisbon, Portugal (cf. legends). (b) Chronograms of the 11-yr running mean anomalies of Lut2004, CalT and
594 Sim1/Sim2 for the period of 1600–1989. The SSA filtered ensemble mean temperature from the two simulations
595 (SSA-trend) is also displayed. The 11-yr running means of InstT (instrumental annual mean temperature)
596 anomalies are depicted for the period of 1901–1999, along with the respective linear trend. Note that anomalies in
597 each series are with respect to their common period (1901–1989).

598
599 **Fig. 3.** Scatterplot between InstT and CalT anomalies over their common period (1901–1989). The corresponding
600 regression line, calibration equation and R-squared measure (determination coefficient) are also pointed out.

601 **Fig. 4.** Chronogram of: (a) CalT – calibrated annual mean temperature – in the period of 1600–1999 and InstT in
602 the period of 1901–1999. Estimated errors are grey shaded, with a mean error of 0.05°C (b) Forward – $u(t)$ – and
603 backward – $u'(t)$ – series of the normalised Kendall τ parameter from the progressive Mann-Kendall analysis of
604 CalT. 95% confidence interval for the no trend hypothesis in grey shading.
605

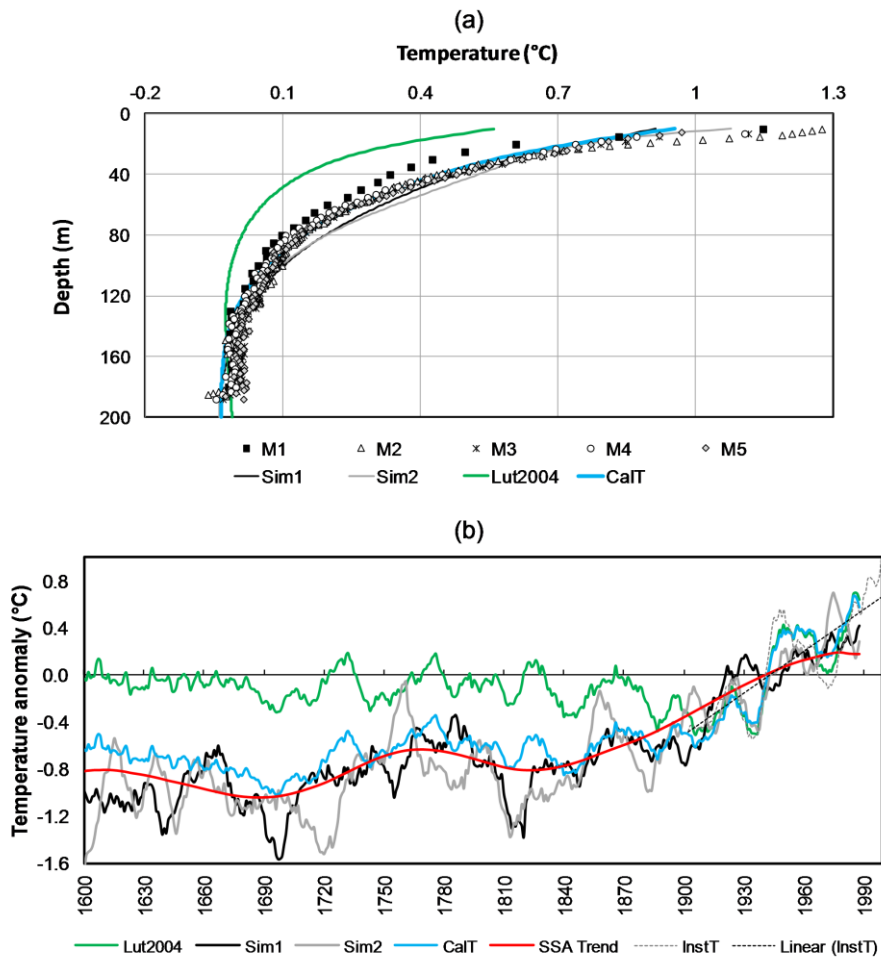
606 **Fig. 5.** Scatterplot of CalT in the period of 1675–1715 as a function of the annual temperature indices. Light (dark)
607 grey circles represent cold (hot) years from documentary evidence. Circles with black edges indicate agreement
608 between the two datasets. Years with ‘0’ index are omitted for the sake of readability of the plot. The horizontal
609 line corresponds to CalT mean. Some labels are omitted for the sake of clarity.

610



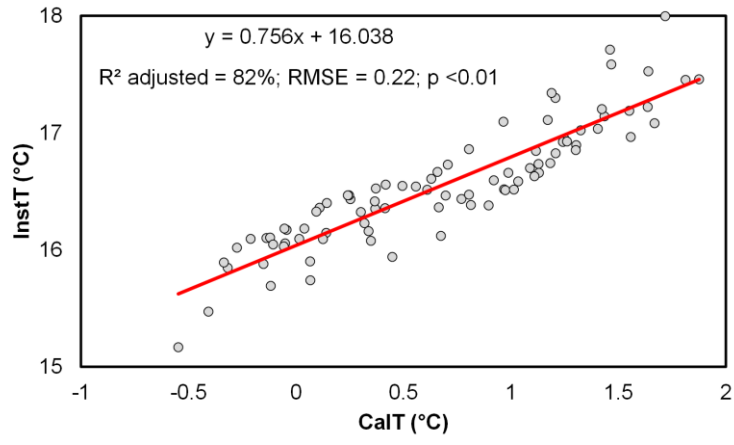
611
612
613

Fig. 1



614
615
616

Fig. 2



617
618
619

Fig. 3

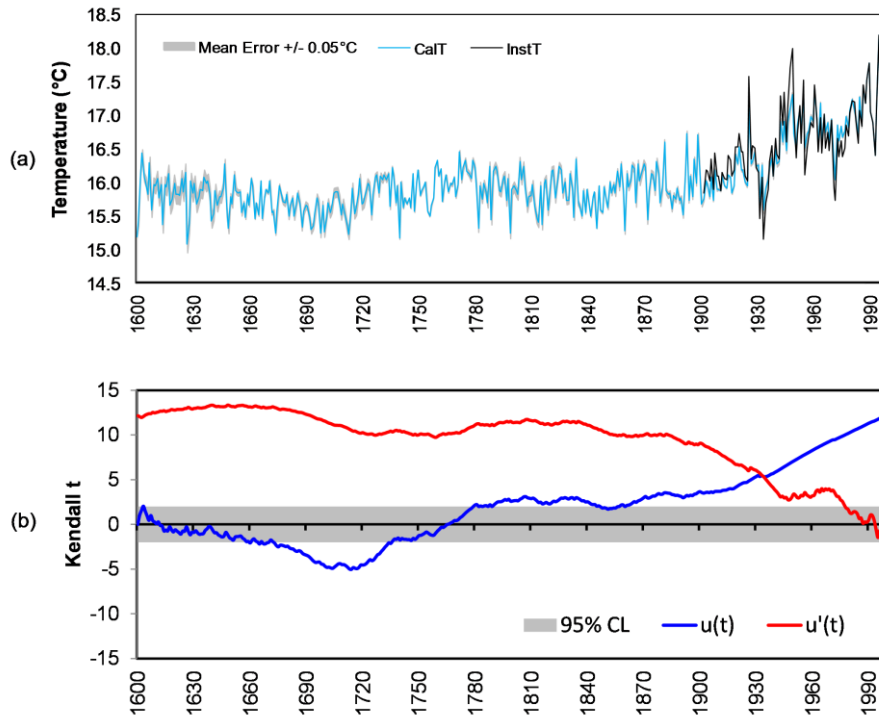
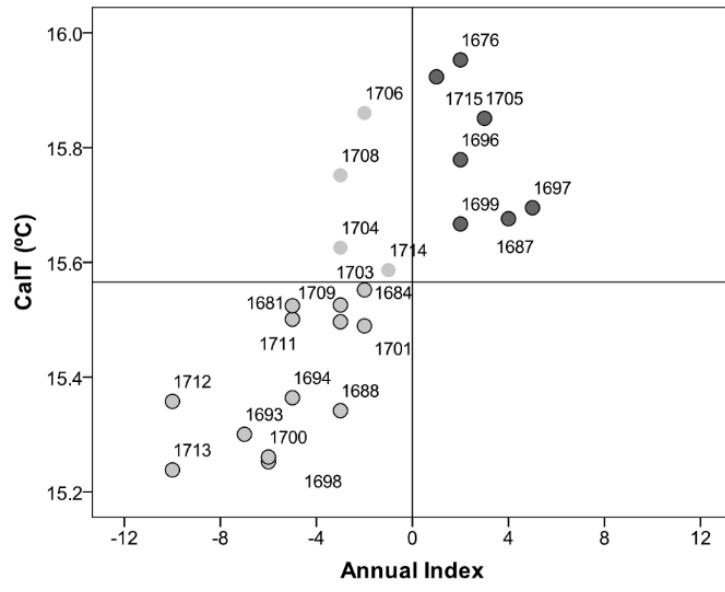


Fig. 4

620
621
622
623

624



625
626
627

Fig. 5